

Article

A Novel Method for Predicting Residual Stress in GH4169 Machined Surfaces through Micro-Hardness Measurement

Gonghou Yao ^{1,2}, Zhanqiang Liu ^{1,2,*}  and Haifeng Ma ^{1,2}

¹ School of Mechanical Engineering, Shandong University, Jinan 250061, China; sduyagonghou@mail.sdu.edu.cn (G.Y.); mahaifeng@sdu.edu.cn (H.M.)

² Key National Demonstration Center for Experimental Mechanical Engineering Education/Key Laboratory of High Efficiency and Clean Mechanical Manufacture of MQE, Jinan 250061, China

* Correspondence: melius@sdu.edu.cn; Tel./Fax: +86-531-88393206

Abstract: The presence of residual stress seriously affects the mechanical performance and reliability of engineering components. Here, the authors propose a novel method to determine corresponding residual stress through micro-hardness measurements of machined surfaces. In this study, a mathematical model with equal biaxial stress indentation is established. Then, the correlation of micro-hardness with indentation and residual stress is used to determine the prediction equation of residual stress. The material applied in this study is the nickel-based Superalloy GH4169. The residual stress prediction formula for Superalloy GH4169 is ultimately determined through the finite element method by subjecting the indentation to residual stress and fitting the experimental test data. The relationship between the indentation modulus and indentation depth is given quantitatively. The relationship between residual stress and hardness is given quantitatively. The prediction results show that the compressive residual stress can enhance the material hardness and make the contact deformation only require a low indentation depth to achieve complete plastic deformation. Conversely, the tensile residual stress can result in a deeper depth and less hardness at the initial stage of the fully plastic state. For the materials that yield more easily (small ratio of elastic modulus to yield strength), the effect is more evident. The model presented in this paper can accurately forecast corresponding residual stress through measurements of the micro-hardness of machined surfaces.

Keywords: residual stress; micro-hardness measurement; finite element modeling; indentation depth



Citation: Yao, G.; Liu, Z.; Ma, H. A Novel Method for Predicting Residual Stress in GH4169 Machined Surfaces through Micro-Hardness Measurement. *Appl. Sci.* **2023**, *13*, 13257. <https://doi.org/10.3390/app132413257>

Academic Editor: Chiara Bedon

Received: 22 November 2023

Revised: 12 December 2023

Accepted: 13 December 2023

Published: 14 December 2023



Copyright: © 2023 by the authors. Licensee MDPI, Basel, Switzerland. This article is an open access article distributed under the terms and conditions of the Creative Commons Attribution (CC BY) license (<https://creativecommons.org/licenses/by/4.0/>).

1. Introduction

Residual stress is the internal stress of an object required in order to maintain macroscopic stability when there is no external force. Machining and heat treatment usually cause residual stress inside a component. The existence of residual stress has a great influence on the service performance and life of a component. Previous research and practical results indicate that adjusting and controlling a machined surface's residual stress through appropriate methods can significantly improve the yield strength, fatigue strength, wear resistance and fracture resistance of a component [1]. Therefore, it is necessary to measure and control the residual stress on machined surfaces through research.

At present, there are many methods for detecting residual stress, such as the drilling method [2,3], strip cutting method [4], contour method [5], neutron diffraction method, X-ray diffraction method, magnetic method [6], etc. But many of them have the disadvantages of long testing time and high cost. Indentation detection is a nondestructive, efficient and low-cost method. Indentation testing can detect a material's properties, for instance, its Young's modulus, yield strength, hardness, tensile strength and work hardening index [7–11]. Indentation detection makes it more convenient to study the dynamic mechanism of component fatigue damage [12–14].

In the past few decades, researchers have found that the indentation of materials before and after indentation experiments is affected by residual stress to different degrees,

and the reasons for this influence have been studied. In 1932, for the first time, Kokubo [15] published a study on changes in the hardness of certain metal or alloy sheets as a result of bending under external loads. Tsui et al. [16] and Bolshakov et al. [17] demonstrated the influence of stress on indentation measurements of elastic modulus and hardness through experiments and FEM simulation analyses, respectively. Both studies showed that the elastic modulus and hardness calculated using the actual contact area measured by an optical microscope were not affected by the residual stress of the workpiece. However, it should be noted that this conclusion was only derived from an aluminum alloy indentation. In 1998, Suresh et al. [18] developed a theoretical model for measuring biaxial residual stress through nano-indentation technology. This model was based on the theory that residual stress does not affect material hardness. The residual stress calculation formula was derived by substituting the impact of residual stress on indentation depth and contact area in the material with uniaxial stress aligned with the load direction of the indenter. Atare et al. [19] evaluated ceramic films' residual stress using the Suresh model and XRD method. The residual stress values of ceramic films indirectly measured by the indentation method deviated significantly from those directly determined by the XRD method. In order to reduce the deviation, Atare modified Suresh's model and proposed a modified residual stress calculation method. Xu et al. [20] conducted a comprehensive investigation on the impact of residual stress on the elastic recovery ratio. They employed extensive finite element simulations to study this phenomenon and presented a detailed calculation model for residual stress. However, this model required the measurement of a large number of parameters at different locations on the workpiece, such as contact area, modulus of elasticity, micro-hardness, etc., for the calculation of residual stresses. Therefore, this model is difficult to use for generalization. Taljat and Pharr [21] performed finite element simulations of spherical indentation models for a variety of ideally elastic or ideally plastic materials under equal biaxial stresses (compressive or tensile stresses). It was found that differences in load–displacement characteristics due to residual stresses have a significant effect on the elastic and elastoplastic phases of the material. Inspired by this, the study proposed a method to calculate residual stresses by measuring the modulus of elasticity, yield stress and indentation load during elastic deformation of the material. All these parameters could be obtained computationally by indentation experiments and finite element simulations. Swadener et al. [22] summarized two different spherical indentation experiments by summarizing and analyzing the results of Taljat and Pharr [21], and summarized two methods for estimating residual stresses. One method was a residual stress calculation method based on yield stress. The other method was to calculate the residual stresses by assessing the deviation of the average contact pressure in the elastoplastic transition zone. In order to facilitate the calculation of residual stresses on a machined surface, Chen et al. [23] analyzed the relationship between the energy required in the indentation process and the residual stresses according to the principle of the conservation of energy from the perspective of the work done by residual stress, and derived a more simple formula for calculating residual stress. In the Vickers indentation cycle, the stress type and its value can be easily calculated using the energy method without any comparison of the load–displacement curve of the non-stressed reference material. Lee et al. [24] proposed a method to measure the value of the residual principal stress component by measuring the deposition height in different directions of the indentation. The assumption made by the model was that there is a linear connection between the residual stress and the highest load when compared to specimens without any stress. Stress-induced load displacements lead to micromechanical contact. The value of the stresses calculated from the contact analysis is nearly of the same magnitude as the stresses applied in the plane. However, when the stresses applied are pure shear stresses, the effect of in-plane stresses on the plastic deformation of the indentation is negligible. Different stress components of the residual stresses result in different deposition heights of the sample along the main direction. The deposition height can be obtained by performing optical microscopy tests on the indentation. However, the disadvantages of this

method are also obvious, it is difficult to accurately measure the height of accumulation and it consumes too much time with related work.

With the continuous development of indentation technology, the indentation method has been widely used in various fields, but it still has disadvantages. If the relationship between residual stress and hardness can be established, using hardness to evaluate the residual stress of materials will help in obtaining a stress measurement and in the monitoring of in-service equipment, so it is necessary to conduct more in-depth research on residual stress measurement by the indentation method. When the indentation method is applied to measure hardness, the surface residual stress will affect the shape and size of the indentation. In indentation experiments for workpiece surface without residual stresses, the purely elastic deformation of elastoplastic prismatic indentations was transformed into plastic yielding when the average pressure in the contact zone increased above its yield stress. Hydrostatic stresses are known to have no effect on the plastic deformation of an indentation. Biaxial compressive residual stresses lead to an increase in the critical mean contact pressure at yielding. Biaxial tensile residual stresses reduce the critical mean contact pressure at yielding. A similar residual stress effect exists in the transition phase from elastic to plastic deformation. When the average contact pressure reaches a maximum value, the indentation deformation transforms into the fully plastic phase. As shown in Figure 1, the hardness of a material increases as the applied compressive residual stress increases. The higher the compressive residual stress, the sooner the indentation changes to a fully plastic state. On the contrary, the higher the tensile residual stress, the lower the hardness of the material and the deeper the indentation needed to obtain a fully plastic state. With the same indenter, the deeper the indentation depth h , the larger the projected surface area of the indentation. In view of this, this study proposed a method to determine the quantitative relationship of hardness with residual stresses by examining the indentation area, and obtained residual stress indirectly through measurements of the micro-hardness of a machined surface. In this study, a theoretical model of positive rhomboid indentation with equal biaxial residual stress was established. Then, the model was modeled by the finite element method. By fitting the simulation and experimental data, the relationships between indentation modulus and indentation depth, residual stress and hardness were quantitatively given. Finally, the residual stress prediction formula of Superalloy GH4169 was obtained. The prediction formula proposed in this study can accurately predict the residual stress on a processed surface by measuring the hardness of the material after determining the required materials. It takes less time and consumes less money, and can also be used as a substitute in the absence of residual stress testing instruments.

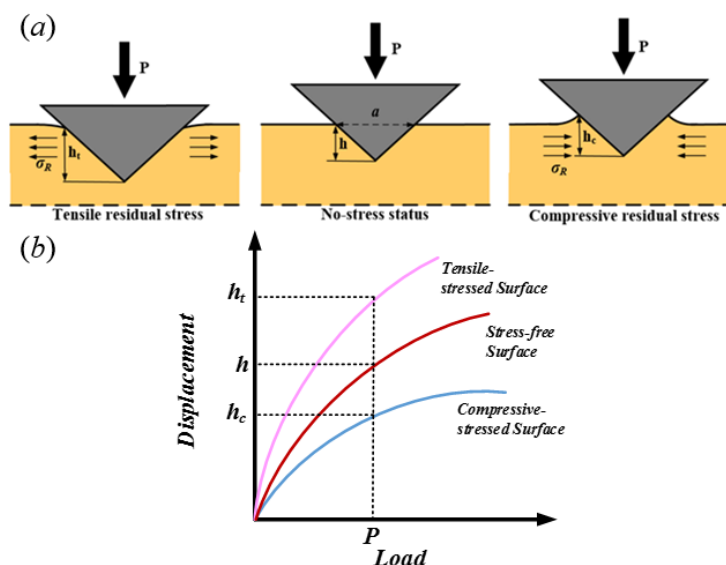


Figure 1. (a) Theoretical surface status around the contact area for indentation states and (b) the influence of residual stress type on the load–displacement curve during indentation circulation.

2. Theoretical Research

The indentation model represents the contact between a deformable semi-infinite matrix and a rigid positive pyramid indenter, as shown in Figure 2. The matrix has equal biaxial residual stress σ_R . The matrix is assumed to be a homogeneous elastoplastic material with yield stress Y . The plastic yield adopts the von Mises criterion. The indentation modulus is $E^* = E/(1 - \nu^2)$. E is defined as the elastic modulus and ν is defined as the Poisson's ratio. Assuming an indenter load of P , which is pressed perpendicular to the surface of the specimen substrate, its orthorhombic indentation depth is λ . The actual contact diagonal length a is extracted considering accumulation or subsidence. Therefore, the average pressure P_m of the entire substrate–indenter contact area is defined as Equation (1),

$$P_m = \frac{2P}{a^2} \tag{1}$$

P_m reaches its maximum value at fully plastic deformation, where the indentation depth is λ^{\max} . The maximum pressure is material hardness H [25,26].

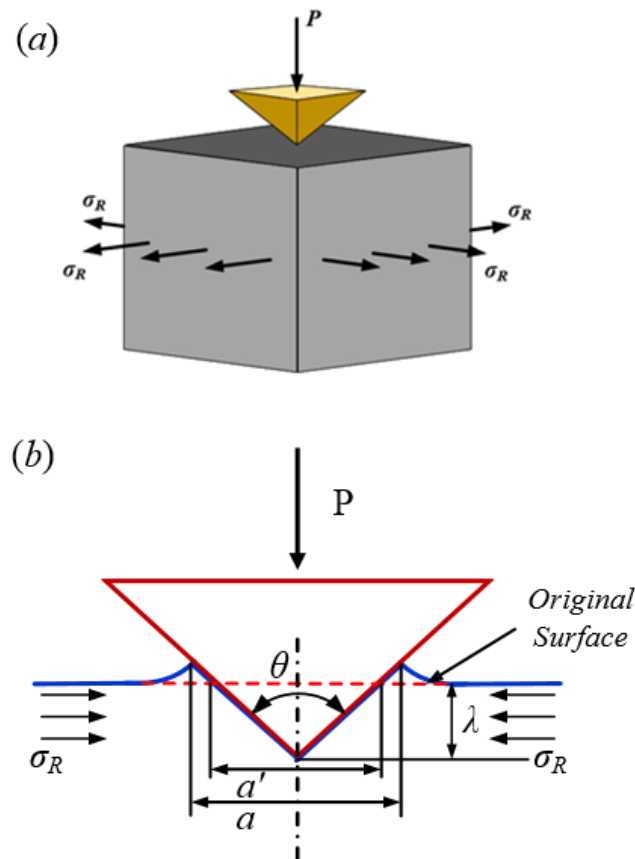


Figure 2. Positive rhomboidal indentation with equal biaxial residual stress: (a) 3D model and (b) 2D indentation.

When there are no residual stresses in the matrix, the hardness of the matrix is H_0 and the corresponding indentation depth of the indenter is λ_0^{\max} . The contact response differences between the materials with residual stress and those without residual stress are defined as $\Delta H = H - H_0$ and $\Delta \lambda^{\max} = \lambda^{\max} - \lambda_0^{\max}$. ΔH and $\Delta \lambda^{\max}$ are the functions of indentation modulus E^* , Poisson's ratio ν , yield strength Y , residual stress σ_R and indenter diagonal length a .

$$\Delta H = H - H_0 = f(\nu, E^*, R, Y, \sigma_R) \tag{2}$$

$$\Delta \lambda^{\max} = \lambda^{\max} - \lambda_0^{\max} = g(\nu, E^*, R, Y, \sigma_R) \tag{3}$$

Because Poisson’s ratio ν has little effect on static indentation, the effect of Poisson’s ratio is not considered in order to simplify the calculations [27,28]. Based on the [1] theorem of dimensional analysis, ΔH and $\Delta\lambda^{\max}$ are represented as

$$\frac{\Delta H}{Y} = \frac{H - H_0}{Y} = f\left(\frac{E^*}{Y}, \frac{\sigma_R}{Y}\right) \tag{4}$$

$$\frac{\Delta\lambda^{\max}}{a} = \frac{\lambda^{\max} - \lambda_0^{\max}}{a} = g\left(\frac{E^*}{Y}, \frac{\sigma_R}{Y}\right) \tag{5}$$

H_0 and λ_0^{\max} can be further simplified and integrated as follows [25]:

$$\frac{H_0}{Y} = b \left[1 - \left(\frac{E^*}{Y}\right)^{-0.05} \right] \tag{6}$$

$$\frac{\lambda_0^{\max}}{a'} = \frac{1}{c \frac{E^*}{Y} + d} \tag{7}$$

where b , c and d are undetermined constant coefficients, which need to be obtained by fitting simulation data. Based on the geometric relationship, the truncated contact diagonal length a' can be calculated from the indentation depth and the angle of indenter:

$$a' = \tan \frac{1}{2}\theta \times \lambda$$

Organizing the above equations, the equation for the relationship between hardness deviation and residual stress can be derived as follows:

$$\frac{H}{Y} - \frac{H_0}{Y} = \left(\frac{E^*}{Y}\right)^{0.5} \times \begin{cases} -B\left(\frac{\sigma_R}{Y}\right)^2 - C\frac{\sigma_R}{Y} \leq 0 \\ D\frac{\sigma_R}{Y} > 0 \end{cases} \tag{8}$$

where H is hardness, Y is yield strength, E^* is indentation modulus and σ_R is residual stress. Coefficients B , C and D are obtained by fitting the simulation and experimental data according to the determination of specific materials.

Equation (8) is further arranged as a relation between residual stress and hardness.

$$\sigma_R = \begin{cases} -\frac{Y}{2B} \times \left(C + \sqrt{C^2 - 4B\left(\frac{E^*}{Y}\right)^{-0.5} \times \left(\frac{H}{Y} - \frac{H_0}{Y}\right)} \right), \sigma_R \leq 0 \\ \left(\frac{E^*}{Y}\right)^{-0.5} \times D(H - H_0), \sigma_R > 0 \end{cases} \tag{9}$$

3. Indentation Finite Element Model

Indentation experiments with additional biaxial compressive or tensile residual stresses were simulated with ABAQUS finite element simulation. A standard Vickers regular pyramid indenter is used in the model, and the angle between the two opposite surfaces is 136° . Due to symmetry, in order to reduce the amount of calculation, a quarter indenter model was adopted for simulation analysis. The matrix size was set at $8\text{ mm} \times 8\text{ mm} \times 8\text{ mm}$, and the maximum indentation depth was 0.6 mm . Because the matrix size was much larger than the indentation depth, the boundary effect could be ignored. The indenter material is much stiffer than the matrix material, so the indenter is simplified into a rigid body. The height of the indenter is 1 mm , and the upper surface side length is 2.5 mm . The mesh division of the model is shown in Figure 3. The matrix is meshed by more than 30000 four-node bilinear axisymmetric quadrilateral elements. The interaction is defined as the frictionless surface contact between the indenter (primary surface) and the specimen (secondary surface). Figure 4 shows the boundary constraints of the simulation model. As shown in Figure 4, the bottom surface of the specimen has the y displacement fixed. The simulation model applies boundary conditions fixed along the centerline to simulate axisymmetric behavior. The residual stress is simulated by applying prestress σ_R to the

matrix along the vertical $-X$ and X directions. Due to the large plastic contact deformation, the finite deformation option was used. The transformation of material was carried out by changing the yield strength and indentation modulus. Figure 5 shows the indentation model results.

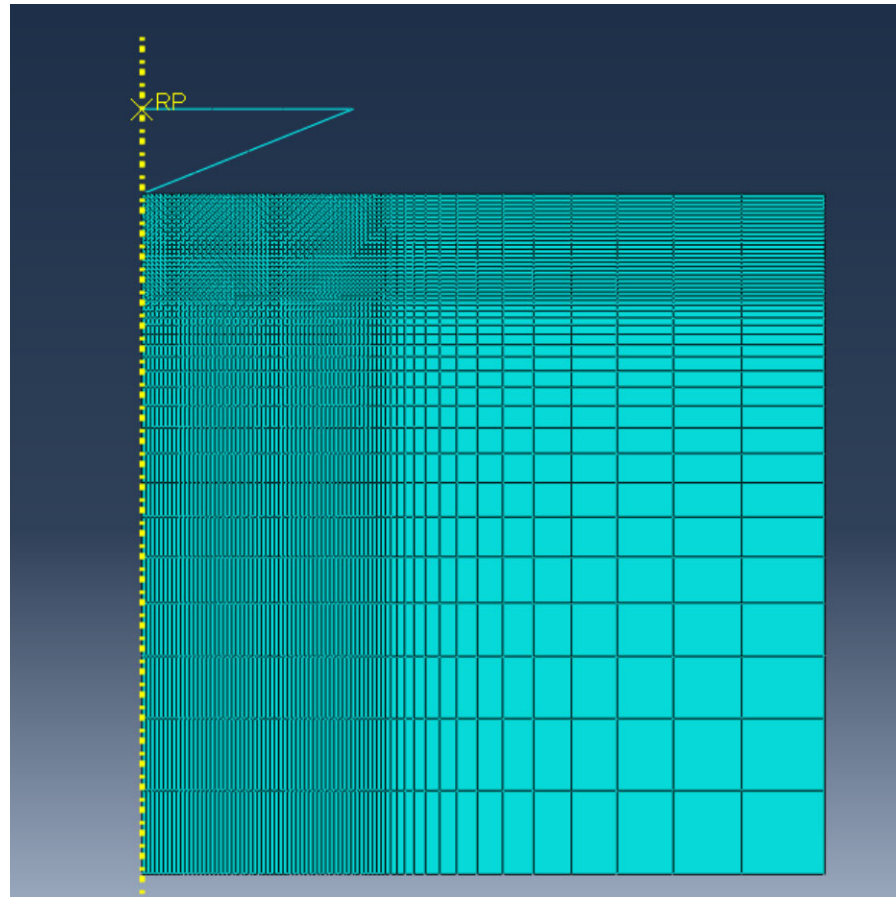


Figure 3. Mesh division of finite element indentation model.

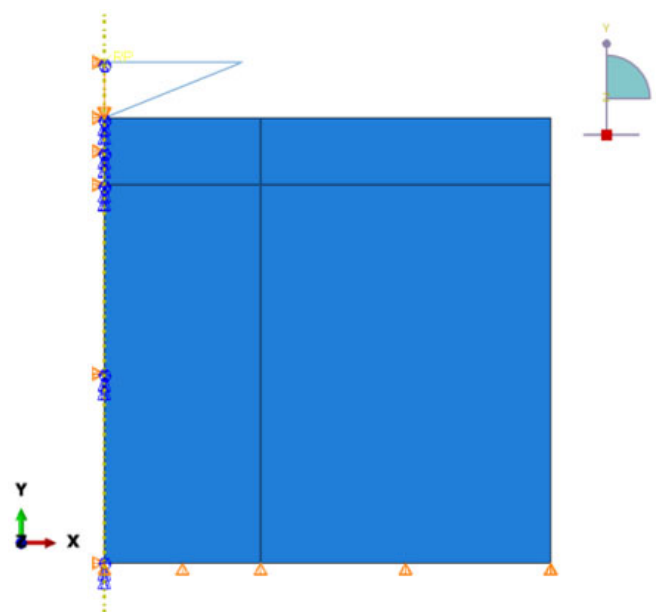


Figure 4. The boundary constraints and loads of the simulation model.

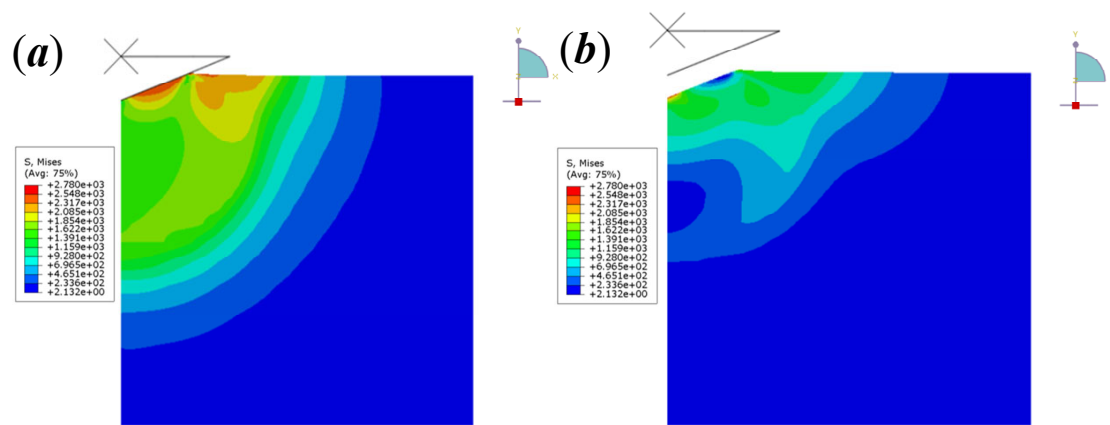


Figure 5. Indentation model results. (a) Indentation at maximum depth and (b) indentation with complete load release.

In order to validate the correctness of the prediction model and the need of this research, the material was identified as Superalloy GH4169. By comparing the theoretical results of residual stress with the test values, the feasibility and accuracy of the prediction model were determined. The Johnson–Cook parameters for GH4169 are listed in Table 1. Table 2 lists the physical and mechanical properties of GH4169.

Table 1. Johnson–Cook constitutive model parameters of GH4169 [29].

A (GPa)	B (GPa)	C	n	m
0.45	1.7	1.7×10^{-2}	0.65	1.3

Table 2. The physical and mechanical properties of GH4169 [30].

Properties	Density	Young’s Modulus	Poisson’s Ratio	Thermal Expansion	Conductivity	Specific Heat
Matrix	8.25×10^3 Kg/m ³	2.1×10^5 GPa	0.305	1.48×10^{-4} m/K	17.8 W/mK	5.263×10^5 J/K

4. Measurements of Hardness and Residual Stress

The experiment was carried out using Superalloy GH4169 as the material. Superalloy GH4169 has excellent high yield strength, tensile strength, temperature resistance and creep cracking strength, so it can be widely used in a variety of demanding applications. Superalloy GH4169 has an austenitic structure consisting mainly of a γ matrix, the dispersed reinforcing phases γ' and γ'' , and a δ phase. The size of the specimen was 10 mm \times 15 mm \times 20 mm. The specimen surface underwent side milling. Figure 6 shows the experimental testing equipment.

The hardness of Superalloy GH4169 side milled surface was measured by a micro-Vickers hardness tester. The indenter of the hardness tester was a diamond cone with an angle of 136°. The micro-hardness test load was 50 g and the hold time was 10 s. In order to avoid the mutual influence of each indentation point, resulting in errors in the measurement data, the measurement distance along the direction of the parallel machined surface was 30 μ m. Each specimen was measured three times, and the average magnitude was taken to indicate the micro-hardness value of the machined surface.

A Pulstec μ -X360n X-ray diffraction stress analyzer was selected to test the residual stresses on the machined surface of the GH4169 specimen. The residual stresses measured in this study were all in the direction of the feed. Each workpiece was measured three times, and the average magnitude was taken to indicate the residual stress value of the machined surface.

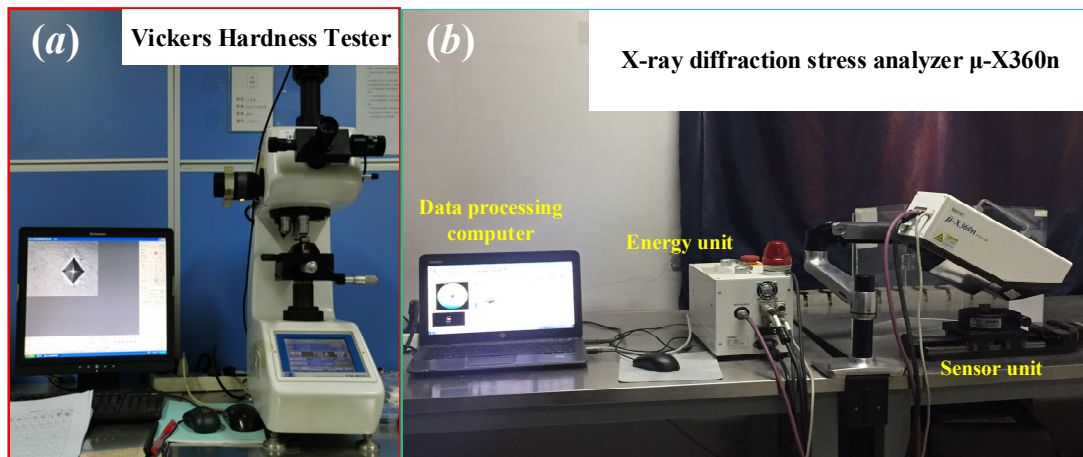


Figure 6. Experimental and testing devices: (a) Vickers Hardness Tester; (b) X-ray diffraction residual stress tester.

5. Results and Discussion

The simulation results show that the load of the indenter was significantly affected by the presence of tensile residual stress. The presence of tensile residual stress resulted in a decrease in the load of the indenter. The larger the residual tensile stress was, the smaller the load of the indenter would be. On the contrary, the greater the compressive residual stress was, the greater the head load would be. This phenomenon could be explained by elastoplastic theory. The residual stress that existed on the surface of the material was parallel to the surface, while the stress that the indenter exerts on the matrix is the compressive stress perpendicular to the machined surface. When tensile stress was present in the workpiece, the plastic deformation capacity of the material was increased, resulting in a reduction in the required indenter load at the same penetration depth.

When $E^*/Y = 245$, the normalized mean contact pressure is affected by the normalized indentation depth, as shown in Figure 7. For different residual stresses, the mean contact pressure has the same variation trend in the elastoplastic zone. With an increase in the normalized indentation depth, the normalized average contact pressure will first show a gradual increasing trend, and then, gradually stabilize, which means that the material has reached a completely plastic state. The critical value of the indentation depth at which the normalized average contact pressure does not change with an increase in the normalized indentation depth is called the critical depth. Different materials have different critical depths, which are related to the physical and mechanical properties of the materials. When the normalized indentation depth reaches the critical depth, the normalized mean contact pressure reaches the maximum value, indicating that the workpiece surface has reached a fully plastic state. When $\sigma_R/Y = 0$, there is no residual stress on the machined surface of the workpiece, and its curve is the curve of contact pressure and indentation depth under ideal conditions. When $\sigma_R/Y < 0$, the material hardness increases with an increase in the compressive residual stress, and the indentation transforms the completely plastic state in advance. The normalized critical indentation depth of the $\sigma_R/Y = -0.8$ curve is about 0.052, while the normalized critical indentation depth of the $\sigma_R/Y = -0.2$ curve is about 0.10. It can be seen that when there is residual compressive stress on the workpiece surface, the greater the compressive residual stress is, the earlier the indentation will transform the fully plastic state. When $\sigma_R/Y > 0$, the material hardness decreases with an increase in the tensile residual stress, and deeper indentation is needed to achieve complete plasticity. The normalized critical indentation depth of the curve $\sigma_R/Y = 0.2$ is about 0.15, while the normalized critical indentation depth of the curve $\sigma_R/Y = 0.8$ is about 0.23. It can be seen that when there is residual tensile stress on the workpiece surface, the greater the residual tensile stress is, the later the indentation will transform the complete plastic state. Comparing the curve $\sigma_R/Y < 0$ with the curve $\sigma_R/Y > 0$, it can be found that the curve

$\sigma_R/Y > 0$ has a larger trend change and contains a wider indentation depth, which also proves that tensile residual stress has a greater influence on indentation than compressive residual stress.

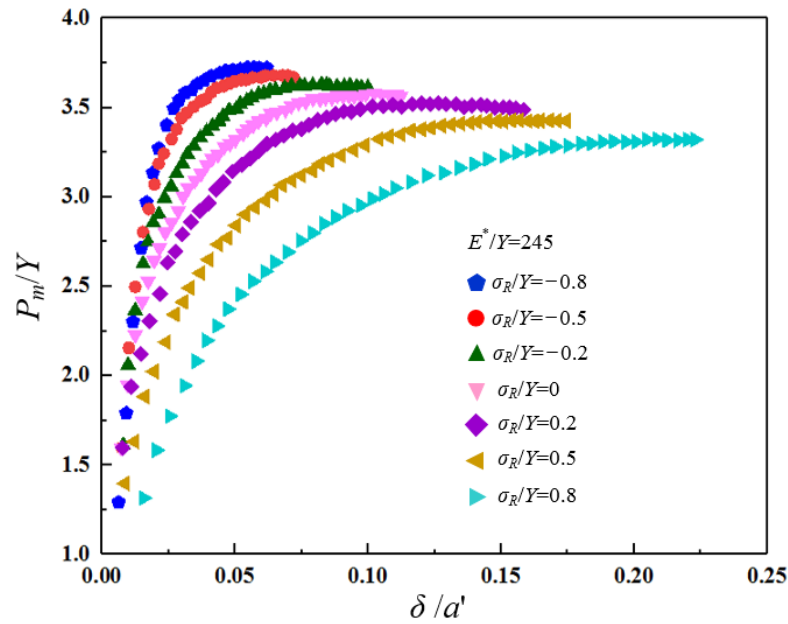


Figure 7. Relationship between normalized depth of indentation and normalized mean contact pressure.

Figure 8 shows the relationship between the simulated normalized hardness difference and residual stress. The relationship curve between the normalized hardness difference and residual stress was obtained by fitting the normalized hardness difference and residual stress data in Figure 8. It can be seen that the curve of normalized hardness difference and residual stress was consistent with Equation (8). When $\sigma_R/Y \leq 0$, the curve of the normalized hardness difference and residual stress was a downward parabola. When $\sigma_R/Y > 0$, the relationship between the normalized hardness difference and residual stress was a downward straight line.

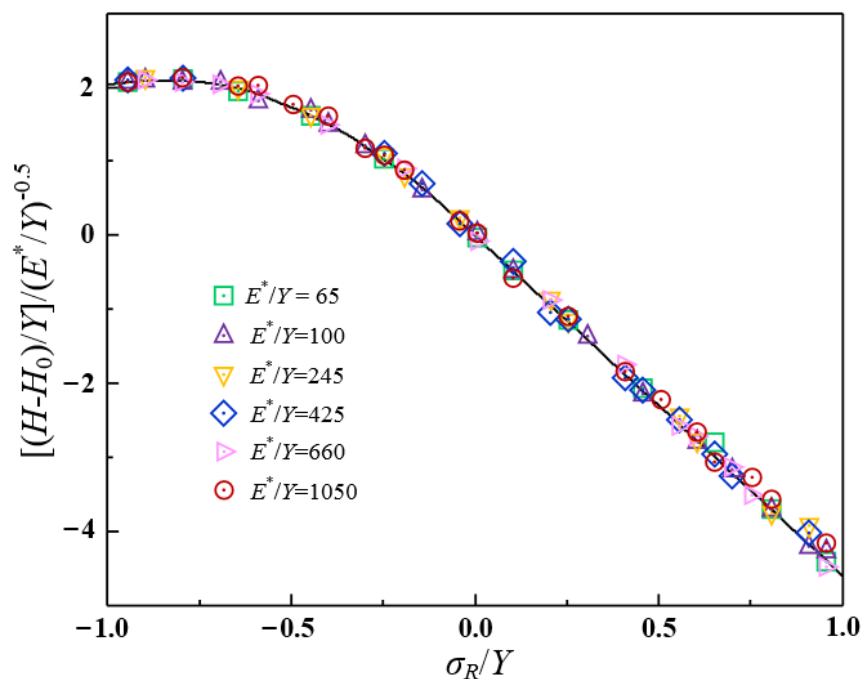


Figure 8. Relationship between normalized hardness difference and residual stress.

The influence of compressive residual stress on hardness was not as significant as that of tensile residual stress. The yield strength of Superalloy GH4169 was about 550 Mpa. When the residual stress exceeded the yield strength of GH4169, the material began to harden and deform, thus increasing the hardness of the sample. Therefore, due to the limitation of applicable conditions, Equation (9) was further modified as follows:

$$\sigma_R = \begin{cases} -\frac{Y}{2B} \times \left(C + \sqrt{C^2 - 4B \left(\frac{E^*}{Y} \right)^{-0.5} \times \left(\frac{H}{Y} - \frac{H_0}{Y} \right)} \right), & -550 \text{ MPa} \leq \sigma_R \leq 0 \\ \left(\frac{E^*}{Y} \right)^{-0.5} \times D(H - H_0), & 0 < \sigma_R \leq 550 \text{ MPa} \end{cases} \quad (10)$$

Tensile residual stresses exist mainly on the machined surface, while compressive residual stresses are found mainly on the machined subsurface [31,32]. The higher the cutting amount, the larger the surface tensile stress [33]. Due to the needs of this funded project, this study mainly focused on the side milling research of Superalloy GH4169. In this study, a side milling experiment of Superalloy GH4169 was carried out, so the residual stresses of the machined surface were all tensile residual stresses. During the experiments, dry cutting was adopted in this study. The milling method was down milling due to the consideration of milling surface quality. Since the influence of tool wear on residual stress was not considered in this research, a new tool was used for each milling. By fitting the simulation and test data, the residual stress prediction formula of this study was fitted as follows:

$$\sigma_R = 51.2(H - H_0), \quad 0 < \sigma_R \leq 550 \text{ MPa} \quad (11)$$

Table 3 lists the hardness test values, measured residual stress values and predicted residual stress values. It can be observed that when the hardness is 443 HV, the percentage difference between the experimental and numerical results is 28.5%. When the hardness is 445 HV, the percentage difference between the experimental and numerical results is 8.1%. When the hardness is 448 HV, the percentage difference between the experimental and numerical results is 15.8%. It can be found that the closer the hardness of the material is to 445 HV, the more accurate the prediction accuracy is. The average percentage difference between the simulation and test results is 17.5%. Figure 9 shows the forecast value and the measured value of the residual stress of the fitted prediction formula. It can be found that the prediction model is more accurate in predicting tensile stress based on hardness, and the prediction accuracy of the prediction model is about 82.5%. Although the method proposed by Lee et al. [24] has the advantage of measuring the component size of residual stress compared with the method proposed in this study, it needs to consider the load–displacement curve in the state without residual stress, it is difficult to accurately measure the height of accumulation and it consumes too much time with related work. Greco proposed a method for estimating the magnitude and direction of non-equal biaxial residual stress components based on indentation [34]. The proposed method utilizes the force penetration response provided by the improved Berkovich tip to improve the prediction accuracy, but it also requires longer testing time and costs more money than the method in this study. At the same time, since the lower limit of the detectable stress zone is very low at high stress levels close to the yield strength, the measurable range of stress decreases sharply with a decrease in residual stress, and finally disappears when the lowest detectable limit of stress is reached.

Table 3. The hardness test values, measured residual stress values and predicted residual stress values.

Sample	Hardness (HV)	Measured Residual Stress (MPa)	Predicted Residual Stress (MPa)	Percentage Difference
1	443 (±2.85)	212 (±3.61)	153.67	28.5%
2	445 (±2.76)	237 (±8.54)	256.12	8.1%
3	448 (±3.47)	354 (±6.24)	409.79	15.8%

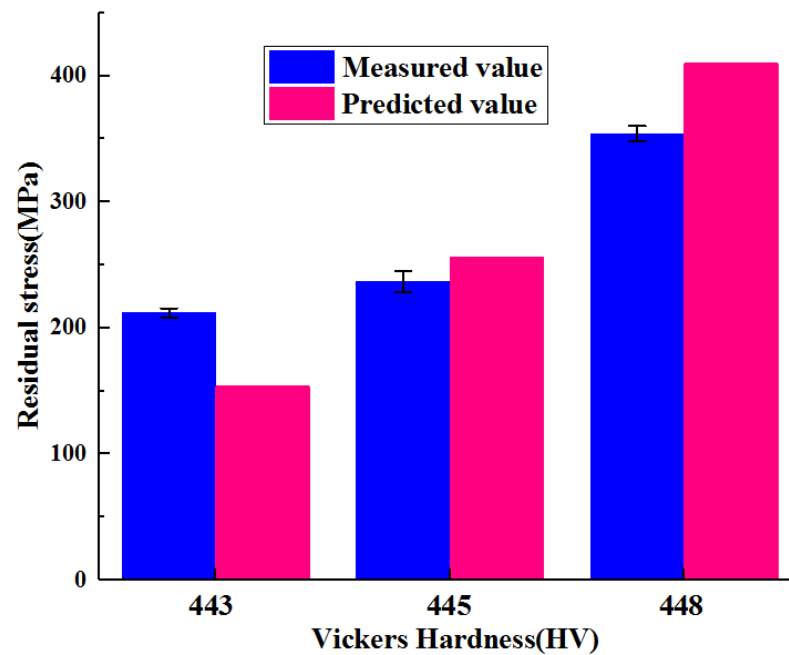


Figure 9. Comparison of tensile stress prediction and measurement.

As mentioned above, Chen et al. [23] proposed a method to calculate the state and magnitude of residual stress through the energy method in the Vickers indentation cycle. The energy contribution to residual stress can be calculated from the indentation approximation with applied equiaxial residual stresses:

$$U_r = \frac{2}{3} (\tan^2 \theta) h_r^3 \sigma_r \quad (12)$$

where U_r is the energy contribution to residual stresses on machined surfaces during indentation cycles, θ is the residual cone half-angle after stabilization of the indentation after complete unloading of the applied load, h_r is the residual displacement after complete unloading in the load–displacement curve and σ_r is the residual stress. The common advantage of the research prediction method proposed in this paper and Chen’s method is that they do not need to consider the solution of the relevant physical quantities of the stress-free state curve of the material. But Chen’s method needed to use 10 physical quantities and was only applicable to a surface with a plasma spray coating. Compared with the method developed in this paper, the calculation of physical quantities was less, with higher precision and wider applicability. At the same time, Chen’s prediction method has an accuracy of less than 75%, which is not as accurate as the precision measurement in this article. Therefore, it is fully proven that the residual stress prediction formula obtained in this paper can achieve more accurate prediction of residual stress by measuring the micro-hardness of the machined surface.

Finally, it should be noted that this method only applies to elastoplastic materials according to traditional continuum mechanics. In an actual indentation experiment, the hardening of the material will also have a great impact on the residual stress of the indentation. In addition, indentations with sub-micro depths can be influenced by various microscopic mechanisms, such as strain gradients, surface effects or grain dislocations. These effects are also the cause of the error between the residual stress prediction model and the actual test values. These effects were ignored in this study but will be considered in future research.

6. Conclusions

In this study, a mathematical model with double equal biaxial stress indentation was established to simulate the indentation state under residual stress, and the numerical

relationship between hardness and residual stress was established. A residual stress prediction formula with unknown hardness was derived and its finite element model was established. The material was identified as Superalloy GH4169 in this study. The main research results of this paper are as follows:

1. Residual stresses have a significant effect on the true hardness of the material (maximum value of the average contact pressure). During the indentation testing process, the variation in residual stresses is mainly reflected in the maximum average contact pressure and its corresponding indentation depth. The compressive residual stress will increase the hardness of the material so that the depth of the indentation required to reach a fully plastic state of contact deformation is reduced. Conversely, the tensile residual stress causes the material to require a deeper depth and less hardness to reach a fully plastic state. This effect is particularly evident for materials with a small ratio of elastic modulus to yield strength.
2. By fitting the simulation and experimental results of specific material parameters, a residual stress prediction formula is obtained in this study to achieve more accurate prediction of residual stress through measurements of the micro-hardness of machined surfaces.

This study provides a residual stress prediction method based on hardness, which provides a new testing method for the convenient and accurate prediction of residual stress in industrial scenarios, and is conducive to the comprehensive evaluation of the service life of related product components.

Author Contributions: G.Y.: methodology, investigation, formal analysis and writing draft. Z.L.: project administration, formal analysis, review and editing. H.M.: supervision, review and editing. All authors have read and agreed to the published version of the manuscript.

Funding: The authors would like to acknowledge the financial support from the National Natural Science Foundation of China (No. 52275444), Shandong Province Key Research and Development Plan (2023JMRH0307), and Taishan Scholar Foundation.

Institutional Review Board Statement: Not applicable.

Informed Consent Statement: Not applicable.

Data Availability Statement: All data and materials used or analyzed during the current study are included in this manuscript. The raw data required to reproduce these findings cannot be shared at this time as the data also form part of an ongoing study.

Conflicts of Interest: The authors declare no conflict of interest. The manuscript has been approved by all authors for publication. This manuscript is original and neither the entire paper nor any part of its content has never been published in other journals. The data and results are true and clear. We guarantee the transparency and objectivity of this research, and strictly abide by the ethical and professional standards of the industry.

References

1. Zhou, J.; Huang, S.; Zuo, L.; Meng, X.; Sheng, J.; Tian, Q.; Han, Y.; Zhu, W. Effects of laser peening on residual stresses and fatigue crack growth properties of Ti-6Al-4V titanium alloy. *Opt. Lasers Eng.* **2014**, *52*, 189–194. [[CrossRef](#)]
2. Seifi, R.; Salimi-Majd, D. Effects of plasticity on residual stresses measurement by hole drilling method. *Mech. Mater.* **2012**, *53*, 72–79. [[CrossRef](#)]
3. Rickert, T. Residual stress measurement by ESPI hole-drilling. *Procedia CIRP* **2016**, *45*, 203–206. [[CrossRef](#)]
4. Tebedge, N.; Alpsten, G.; Tall, L. Residual-stress measurement by the sectioning method: A procedure for residual-stress measurements by the sectioning method is described. Two different hole-drilling methods were performed and the results are compared. *Exp. Mech.* **1973**, *13*, 88–96. [[CrossRef](#)]
5. Prime, M.B. Cross-sectional mapping of residual stresses by measuring the surface contour after a cut. *J. Eng. Mater. Technol.* **2001**, *123*, 162–168. [[CrossRef](#)]
6. Withers, P.J.; Bhadeshia, H.K.D.H. Residual stress. Part 1—measurement techniques. *Mater. Sci. Technol.* **2001**, *17*, 355–365. [[CrossRef](#)]
7. Wang, S.; Zhao, H. Low temperature nanoindentation: Development and applications. *Micromachines* **2020**, *11*, 407. [[CrossRef](#)]

8. Golovin, Y.I. Nanoindentation and mechanical properties of materials at submicro-and nanoscale levels: Recent results and achievements. *Phys. Solid State* **2021**, *63*, 1–41. [[CrossRef](#)]
9. Ma, Z.; Pathegama Gamage, R.; Zhang, C. Application of nanoindentation technology in rocks: A review. *Geomech. Geophys. Geo-Energy Geo-Resour.* **2020**, *6*, 60. [[CrossRef](#)]
10. Bhushan, B. Depth-sensing nanoindentation measurement techniques and applications. *Microsyst. Technol.* **2017**, *23*, 1595–1649. [[CrossRef](#)]
11. Maletta, C.; Furgiele, F.; Sgambitterra, E.; Callisti, M.; Mellor, B.G.; Wood, R.J.K. Indentation response of a NiTi shape memory alloy: Modeling and experiments. *Frat. Integrità Strutt.* **2012**, *6*, 5–12. [[CrossRef](#)]
12. Sgambitterra, E.; Maletta, C.; Furgiele, F. Investigation on crack tip transformation in NiTi alloys: Effect of the temperature. *Shape Mem. Superelasticity* **2015**, *1*, 275–283. [[CrossRef](#)]
13. Sgambitterra, E.; Maletta, C.; Furgiele, F. Temperature dependent local phase transformation in shape memory alloys by nanoindentation. *Scr. Mater.* **2015**, *101*, 64–67. [[CrossRef](#)]
14. Carmine, M.; Fabrizio, N.; Emanuele, S.; Franco, F. Analysis of fatigue damage in shape memory alloys by nanoindentation. *Mater. Sci. Eng. A-Struct. Mater. Prop. Microstruct. Process.* **2017**, *684*, 335–343. [[CrossRef](#)]
15. Kokubo, S. On the change in hardness of a plate caused by bending. *Sci. Rep. Tohoku Imp. Univ.* **1932**, *21*, 256–267.
16. Tsui, T.Y.; Oliver, W.C.; Pharr, G.M. Influences of stress on the measurement of mechanical properties using nanoindentation: Part I. Experimental studies in an aluminum alloy. *J. Mater. Res.* **1996**, *11*, 752–759. [[CrossRef](#)]
17. Bolshakov, A.; Oliver, W.C.; Pharr, G.M. Influences of stress on the measurement of mechanical properties using nanoindentation: Part II. Finite element simulations. *J. Mater. Res.* **1996**, *11*, 760–768. [[CrossRef](#)]
18. Suresh, S.; Giannakopoulos, A.E. A new method for estimating residual stresses by instrumented sharp indentation. *Acta Mater.* **1998**, *46*, 5755–5767. [[CrossRef](#)]
19. Atar, E.; Sarioglu, C.; Demirler, U.; Kayali, E.S.; Cimenoglu, H. Residual stress estimation of ceramic thin films by X-ray diffraction and indentation techniques. *Scr. Mater.* **2003**, *48*, 1331–1336. [[CrossRef](#)]
20. Xu, Z.H.; Li, X. Influence of equi-biaxial residual stress on unloading behaviour of nanoindentation. *Acta Mater.* **2005**, *53*, 1913–1919. [[CrossRef](#)]
21. Taljat, B.; Pharr, G.M. Measurement of residual stresses by load and depth sensing spherical indentation. *MRS Online Proc. Libr.* **1999**, *594*, 519. [[CrossRef](#)]
22. Swadener, J.G.; Taljat, B.; Pharr, G.M. Measurement of residual stress by load and depth sensing indentation with spherical indenters. *J. Mater. Res.* **2001**, *16*, 2091–2102. [[CrossRef](#)]
23. Chen, Y.; Liu, W.W.; Qi, F. Developed Numerical Investigation into Residual Stress by Vickers Instrumented Indentation Technique. *Appl. Mech. Mater.* **2015**, *719*, 38–45. [[CrossRef](#)]
24. Lee, Y.H.; Kwon, D. Estimation of biaxial surface stress by instrumented indentation with sharp indenters. *Acta Mater.* **2004**, *52*, 1555–1563. [[CrossRef](#)]
25. Kogut, L.; Komvopoulos, K. Analysis of the spherical indentation cycle for elastic–perfectly plastic solids. *J. Mater. Res.* **2004**, *19*, 3641–3653. [[CrossRef](#)]
26. Song, Z.; Komvopoulos, K. Elastic–plastic spherical indentation: Deformation regimes, evolution of plasticity, and hardening effect. *Mech. Mater.* **2013**, *61*, 91–100. [[CrossRef](#)]
27. Chen, X.; Yan, J.; Karlsson, A.M. On the determination of residual stress and mechanical properties by indentation. *Mater. Sci. Eng. A-Struct. Mater. Prop. Microstruct. Process.* **2006**, *416*, 139–149. [[CrossRef](#)]
28. Mesarovic, S.D.; Fleck, N.A. Spherical indentation of elastic–plastic solids. *Proc. R. Soc. Lond. Ser. A Math. Phys. Eng. Sci.* **1999**, *455*, 2707–2728. [[CrossRef](#)]
29. Uhlmann, E.; Von Der Schulenburg, M.G.; Zettler, R.J.C.A. Finite element modeling and cutting simulation of Inconel 718. *CIRP Ann.* **2007**, *56*, 61–64. [[CrossRef](#)]
30. Yao, G.; Liu, Z.; Song, Q.; Wang, B.; Cai, Y. Numerical prediction and experimental investigation of residual stresses in sequential milling of GH4169 considering initial stress effect. *Int. J. Adv. Manuf. Technol.* **2022**, *119*, 7215–7228. [[CrossRef](#)]
31. Yang, S.; Jin, X.; Engin, S.; Kountanya, R.; El-Wardany, T.; Lee, S.Y. Effect of cutting fluids on surface residual stress in machining of waspaloy. *J. Mater. Process. Technol.* **2023**, *322*, 118170. [[CrossRef](#)]
32. Strodick, S.; Schmidt, R.; Biermann, D.; Zabel, A.; Walther, F. Influence of the cutting edge on the surface integrity in BTA deep hole drilling—Part 2: Residual stress, microstructure and microhardness. *Procedia CIRP* **2022**, *108*, 276–281. [[CrossRef](#)]
33. Berruti, T.; Lavella, M.; Gola, M.M. Residual stresses on Inconel 718 turbine shaft samples after turning. *Mach. Sci. Technol.* **2009**, *13*, 543–560. [[CrossRef](#)]
34. Greco, A.; Sgambitterra, E.; Furgiele, F. A new methodology for measuring residual stress using a modified Berkovich nano-indenter. *Int. J. Mech. Sci.* **2021**, *207*, 106662. [[CrossRef](#)]

Disclaimer/Publisher’s Note: The statements, opinions and data contained in all publications are solely those of the individual author(s) and contributor(s) and not of MDPI and/or the editor(s). MDPI and/or the editor(s) disclaim responsibility for any injury to people or property resulting from any ideas, methods, instructions or products referred to in the content.